*Journal of Environmental Sciences* Vol. 5, No.3, pp. 351－366 ISSN 1001-0742

# Kinetics of hydrogen peroxide-sulfur (IV) reaction in atmospheric precipitation*

Bai Chunhong, Huang Meiyuan, Shen Zhilai

Institute of Atmospheric Physics, Chinese Academy of Sciences, Beijing 100029, China

Shen Ji, Ma Rusen

Research Center for Eco-Environmental Sciences,
Chinese Academy of Sciences, Beijing 100085, China

**Abstract**— The kinetics of the reaction of dissolved S(IV) with $H_2O_2$ was studied on 59 precipitation samples collected in Southwestern China, during the period of June 1988 to October 1989, from which the oxidation rates of the reaction were measured. The extent of reaction was followed by continuous amperometric measurement of the concentrations of the reagents. The two systems (i. e. rainwater and purified water) have been studied with the same methodology under identical reaction conditions (e. g. reagent concentrations, ionic strength and temperature). The kinetics was studied in no buffer solutions. The effect of formaldehyde on the reaction has also been studied, including kinetic studies in laboratory and model calculations, and it is indicated that formaldehyde with typical atmospheric concentration exerts no influence on the reaction of dissolved S(IV) with $H_2O_2$. In addition, the activation energy of the reaction was also measured in purified water as reaction medium for temperature range 0－50 ℃ at pH 4.0.

**Keywords:** hydrogen peroxide; sulfur (IV); formaldehyde; kinetics; atmospheric precipitation.

## 1 Introduction

Acid rain is one of the important environmental issue which is the focus of world attention today. One important pathway to form acid rain is the oxidation of atmospheric $SO_2$ in aqueous phase to form sulfuric acid. According to laboratory kinetic studies and atmospheric concentration measurements hydrogen peroxide has been postulated to be the key atmospheric oxidant for dissolved sulfur (IV) at pH values less than 5 (Lee, 1986). The overall reaction for this oxidation may be written as

$$S(IV) + H_2O_2\ (aq) \xrightarrow{k^{(2)}} S(VI), \qquad (1)$$

* This study was supported by the National Natural Science Foundation of China.

where S(IV) represents the totality of dissolved S(IV) species (i. e. $SO_2(aq)+HSO_3^-+SO_3^{2-}$). The rate of reaction (1) is the first order with respect to each of the reagents, $H_2O_2$ and S(IV), i. e.

$$-d[H_2O_2]/dt = k^{(2)}[H_2O_2][S(IV)], \quad (2)$$

where $k^{(2)}$ is the apparent second-order rate constant.

In order to evaluate the contribution of this reaction to the acidification of precipitation, we have studied the kinetics of the reaction and the effect of formaldehyde on the reaction.

## 2 Experimental section

### 2.1 Material and apparatus

Principal material included:

2.1.1 (1) Horseradish peroxidase, 250 unit/mg enzyme; (2) P-hydroxyphenylacetic acid (PHOPAA); (3) Tris-(hydroxymethyl) aminomethane (TRIS), reagent grade; (4) 30% hydrogen peroxide, reagent grade; (5) Deionized water made by Institute of Semiconductor, Chinese Academy of Sciences (conductivity $<1\times10^{-6}$).

Principal apparatus: amperometric instrument (self-made).

In which (1), (2) and (3) three materials were used in $H_2O_2$ analysis.

2.1.2 Reagent apparatus

Fig. 1 is the schematic diagram of the experimental set up. Major part included thermostat, amperometric instrument which was used to follow the extent of reaction and recorder instrument which recorded signals.

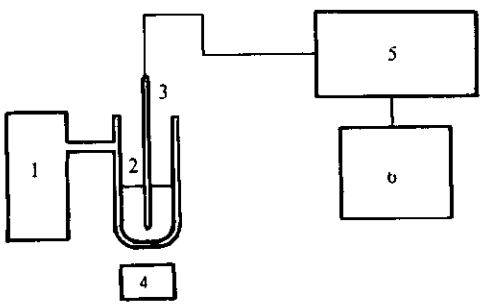


The glass reaction vessel(volume 50ml) was equipped with a water jacket for temperature control, constant temperature (within 25±0.1 ℃ ) was maintained by a bath circulator. The reaction solution was continuously stirred by a magnetic stirrer.

Fig. 1 Schematic diagram of the experimental set up
1. Thermostat 2. Reaction vessel
3. Pt-Ag electrode 4. Stirrer
5. Amperometric device 6. Strip-chart recorder

2.1.3 Solution concentration

2.1.3.1 Standard $H_2O_2$ solution

The standard $H_2O_2$ solution was available by diluting 30% hydrogen peroxide several times. The standard $H_2O_2$ stock solution of 1% concentration was made up for future use, to which $5-10^{-5}$ mol/L $Na_2SnO_3$ was added; the decomposition rate of $H_2O_2$ in this solution was less than 0.13% per month. The standard $H_2O_2$ stock solution was titrated by potassium permanganate ($KMnO_4$) which was titrated by $Na_2C_2O_4$. Standard $H_2O_2$ solution used as the kinetic experiments was made up from the standard $H_2O_2$ stock solution every day.

2.1.3.2 $NaHSO_3$ solution

The content of $NaHSO_3$ in reagent was titrated by iodine method. The solution of $NaHSO_3$ used as the kinetic experiments must be made up every day.

2.1.4 Experimental procedures

The procedures of the kinetic experiment involved the following steps:

Precipitation samples collected were analysed for pH and hydrogen peroxide concentration.

Fresh working solutions of 500$\mu$mol/L $H_2O_2$ and 500$\mu$mol/L $NaHSO_3$ were prepared before conducting kinetics experiments.

After 15 ml rainwater sample was transferred into the reaction cell, 0.15 ml 1mol/L KCl solution was added to adjust the ionic strength to yield [KCl]=0.01 mol/L. Then Pt-Ag/electrode pair was placed in the reaction cell and allowed solution to equilibrate for 5 – 10 minutes.

The "sensitivity" and "zero" controls of the amperometric device were adjusted to yield optimal sensitivity and baseline stability.

For samples that already contained 4 $\mu$mol/L or more of total peroxide, no additional $H_2O_2$ was used. For samples containing less than 4 $\mu$mol/L of peroxide, enough $H_2O_2$ was added to the solution to give a total peroxide concentration of 4 $\mu$mol/L.

A known volume of dilute $NaHSO_3$ solution ($5\times10^{-4}$ mol/L) was added to initiate the reaction.

Kinetic studies of Reaction (1) were conducted with purified water as control experiments, in which HCl and KCl were employed to adjust solution pH and ionic strength. Initial concentrations of $H_2O_2$ and $NaHSO_3$ used were 4.0$\mu$mol/L each. The rate constants of Reaction (1) were determined for pH range 3.1 – 5.2 at $\mu=1\times10^{-2}$ mol/L. The activation energy of Reaction (1) was determined for temperature range 0 – 50 ℃ at $\mu=1\times10^{-2}$ mol/L.

2.1.5 Kinetic measurement and reaction kinetics of $H_2O_2$ with S(IV)

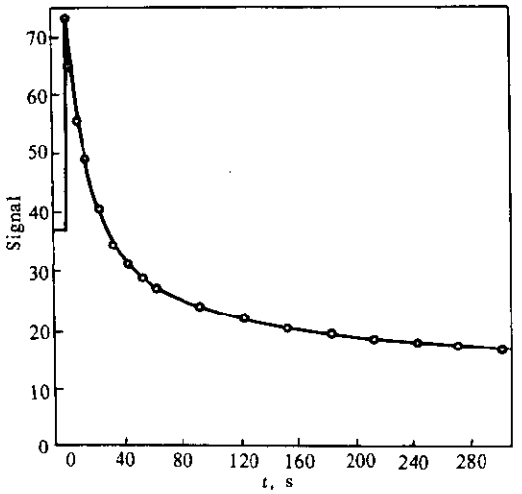


Fig. 2 A typical trace of $H_2O_2$-S (IV) kinetic run, as monitored by the amperometric device. Reaction conditions: $[H_2O_2]_0=[S(IV)]_0=4\times10^{-6}$ mol/L, pH=3.91 and $t=25.0\pm0.1$ ℃

The kinetics of Reaction(1) was studied by following the disappearance of $H_2O_2$ in a reaction mixture as a function of time, using the amperometric instrument. The response time of the instrument varies with ionic strength, in order to ensure that the measurement of reaction kinetics was not affected by the instrument r sponse time, the ionic strength of the samples was adjusted to 0.01mol/L by addition of KCl.

Fig. 2 is a typical trace of $H_2O_2$-S (IV) kinetic run, as monitored by the amperometric device.

The integrated rate laws for a second-order kinetics are for $[H_2O_2]\neq[S(IV)]_0$

$$\frac{1}{[H_2O_2]_0-[S(IV)]_0}\ln\frac{[S(IV)]_0\,[H_2O_2]}{[H_2O_2]_0\,[S(IV)]}=k^{(2)}t, \tag{3}$$

and for $[H_2O_2]_0=[S(IV)]_0$.

$$\frac{1}{[H_2O_2]}-\frac{1}{[H_2O_2]_0}=k^{(2)}t, \tag{4}$$

where the subscript 0 denotes $t=0$. In order to determine $k^{(2)}$, the left-hand function was plotted as a function of $t$. A straight line should result and the slope is equivalent to $k^{(2)}$. Depending on the reaction condition, the data points calculated from the primary signal according to either Eq. (3) or Eq. (4) were analysed using the least squares method. Fig. 3 gives typical plots of the amperometric signal and $[H_2O_2]^{-1}$ as a function of time. The curve shows the time dependence of the total signal accompanying the reaction. The individual points represent calculated values of the function, i. e., $[H_2O_2]^{-1}$ or $\ln([S(IV)]_0[H_2O_2]_0/[H_2O_2]_0[S(IV)])$. The solid straight line is the regression line showing the best fit.

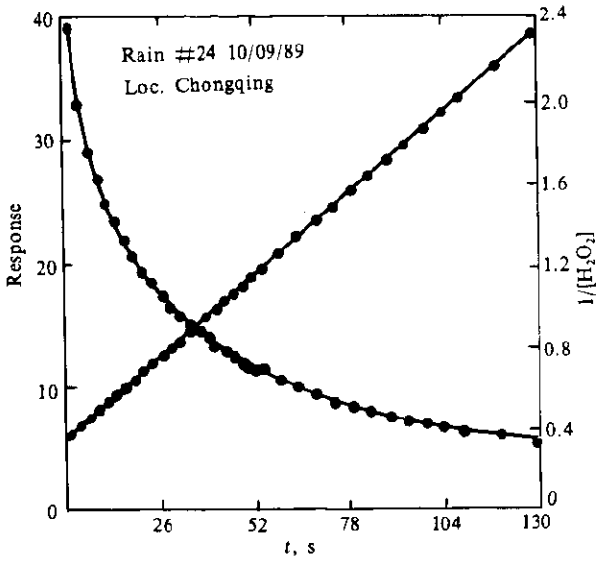


Fig. 3 The amperometric signal and $[H_2O_2]^{-1}$ as a function of time
The curve (left ordinate) represents the amperometric signal decay accompanying the reaction; the straight line (right ordinance) is the best fit to Equation (4) of the data points

## 3 Results and discussion

### 3.1 The pH dependence of rate constant

#### 3.1.1 Purified water study

The rate constants $k^{(2)}$ as a function of pH determined for Reaction (1) in purified water at $\mu = 1 \times 10^{-2}$ mol/L and $t = 25.0 \pm 0.1$ ℃ with $[H_2O_2]_0 = [S(IV)]_0 = 4\mu$mol/L are shown in Fig. 4. The linear regression relation $\log k^{(2)} = (8.05 + 0.03) - (1.006 + 0.006)$ pH; which cover the pH range 3.07−5.18, showed that it can be fitted to a straight line with a slope of −1, consistent with a specific acid-catalyzed reaction of $H_2O_2$ and $HSO_3^-$. Such a pH dependence allows Eq. (2) to be rewritten as

$$-\frac{d[H_2O_2]}{dt} = k^{(3)}[H^+][H_2O_2][S(IV)], \quad (5)$$

from which the pH-independent third-order rate constant $k^{(3)}$ $(= k^{(2)} / [H^+])$ was determined to be $(1.06 + 0.05) \times 10^8$ $(mol/L)^{-2}S^{-1}$.

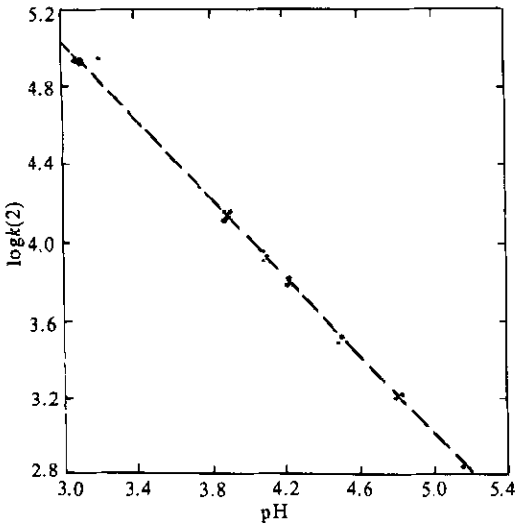


Fig. 4 The pH dependence of the second-order rate constant of Reaction (1), determined by using purified water; $\mu = 0.01$mol/L and $t = 25.0 \pm 0.1$ ℃

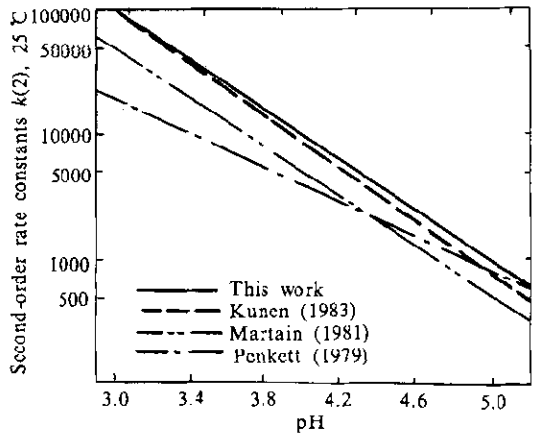


Fig. 5 The second-order rate constants for S(IV) oxidation by $H_2O_2$ at different pH

Fig. 5 shows the second order rate constants for the oxidation of S(IV) by $H_2O_2$ measured in our laboratory. This line is plotted along with lines of Kunen *et al.* (Kunen, 1983), Martainand *et al* (Martainand, 1981) and Penkett *et al.* (Penkett, 1979). The data from the three authors above had been corrected to 25 ℃ by Kunen *et al.* with the Arehenius equation and the activation energy of 30.39 kJ. $mol^{-1}$ given by Penkett *et al.*

It is shown in Fig. 5 that the slopes of lines except that of Penkett *et al.* are approximately equal to $-1$. The rate constants of Martin and Damschen are slightly lower, which obtained by using extension method because their pH range was from 0 to 3, which was lower than the cloud water pH. The slope of Penkett *et al.* line was less than $-1$, inconsistent with HE mechanism (John, 1985). Because Penkett *et al.* studied the kinetics in acetic acid buffer solution, their rate constants might be incredible. The kinetics of this work and Kunen *et al.* were studied in no buffer solution, and pH ranges were both within cloud water pH range (this work was $3.07-5.18$, the latter was $4.0-5.8$), therefore, our rate constants along with the results of Kunen *et al.* might be more credible within cloud water pH range. It is shown in Fig. 5 that our linear very near to the one of Kunen *et al.*, the third order rate constant of the latter $k^{(3)} = (8.03 \pm 0.81) \times 10^7$ $(mol/L)^{-2}S^{-1}$ (22 ℃ ) was also near

to $k^{(3)}=9.03\times10^{7}$ $(mol/L)^{-2}S^{-1}$ (25 ℃) when corrected by activation energy of 28.82 $kJ.mol^{-1}$ measured in our laboratory.

3.1.2 Rainwater study

The second-order rate constants $k^{(2)}$ as a function of pH for rainwater samples are shown in Fig. 6 from 59 samples, which cover the pH range 3.69−5.63, also showed a strong pH dependence, with a slope approximately −1, a linear regression using the least square method yield the relation, $\log k^{(2)}=(7.83\pm0.09)-(0.953\pm0.020)$ pH ($n=59$, $r=-0.988$). The uncertainties indicated here are standard deviation. A single-parameter equation is suggested to the pH dependence for acid-catalyzed reactions.

$$\text{Log } k^{(2)}=\log k^{(3)}-\text{pH}, \tag{6}$$

i. e., the slope is fixed to −1 and the intercept is $\log k^{(3)}$. Fitting the second-order rate constants $k^{(2)}$ determined in rainwater data set to Eq. (6) yield $\log k^{(3)}=(8.04\pm0.07)$ or $k^{(3)}=(1.10\pm0.19)\times10^{8}$ $(mol/L)^{-2}S^{-1}$, the best fit being represented by the dotted line (Fig. 6). The uncertainty given for $\log k^{(3)}$ is the square root of the variance about the best fit to Eq. (6).

It should be noted that the rainwater data exhibited a significant scatter compared to that of purified water, that is ±17.3% vers s ±4.7%; the avcrage rate constant determined in rainwater is 4% higher than that of purified water at the same pH range and ionic strength in our laboratory; the difference of average value is small compared to the scatter exhibited by the data.

Because the average rate constant determined in rainwater samples is identical to that determined in purified water within the experimental error, the small positive bias observed on the kinetics of this reaction is not expected to exert an appreciable effect on atmospheric $SO_2$ oxidation. The rate constants for $H_2O_2$-S(IV) reaction, determined in purified water, used in model calculations is therefore justified.

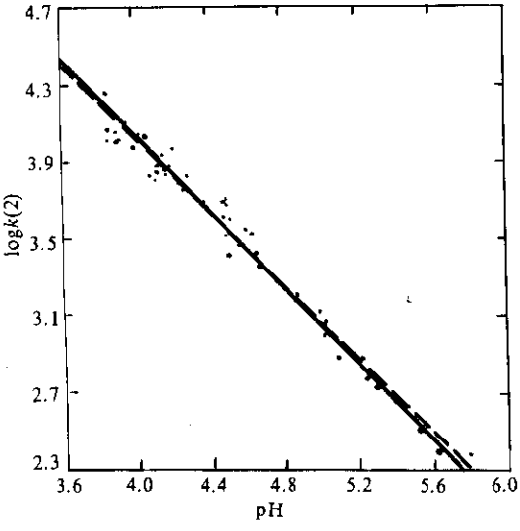


Fig. 6 Second-order rate constant of $H_2O_2$-S(IV) reaction
$\mu=0.01$mol/L, $t=25.0\pm1$ ℃.
The solid line and the dotted line represent measurements of Reaction (1) in purified water and in rainwater respectively

3.2 The activation energy of $H_2O_2$-S(IV) reaction

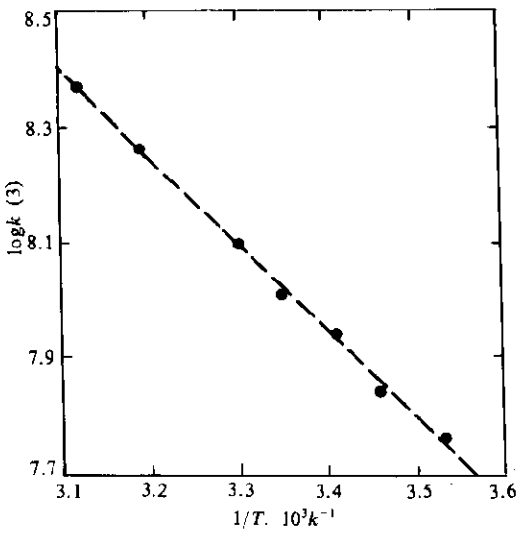


Fig. 7 The temperature dependence of the third-order rate constant of Reaction (1), determined in purified water; $\mu$=0.01mol/L and pH=4.0

The third-order rate constants $k^{(3)}$ determined for $H_2O_2$-S(IV) reaction in purified water at $\mu$=0.01 mol/L and pH=4.0 with $[H_2O_2]_0=[S(IV)]_0=4$ $\mu$mol/L are shown in Fig. 7 as a function of temperature.

The relation between $k^{(3)}$ and temperature is

$$\log k^{(3)}=\log A-\frac{E_a}{2.303R}\cdot\frac{1}{T}, \qquad (7)$$

where $E_a$ is the apparent activation energy of Reaction (1), $R$ is universal gas constant 8.314 J. $mol^{-1}$. $K^{-1}$.

The linear intercept and slope was log $A$=13.1 and −1.505 respectively, from which the activation energy $E_a$=28.82 kJ. $mol^{-1}$ was obtained.

Therefore, the effect of temperature on $H_2O_2$-S(IV) reaction can be represented by the following formula when pH=4.0.

$$\log\ k^{(3)}=k_{298}.\exp[-\frac{E_a}{R}(\frac{1}{T}-\frac{1}{298})],\ (mol/L)^{-2}S^{-1}, \qquad (8)$$

where $k_T^{(3)}$ represents the third-order rate constant at temperature $T$ (K), $k_{298}^{(3)}$ represents the third-order rate constant at temperature 298 (K), $k_{298}^{(3)}=1.02\times10^8$ $(mol/L)^{-2}S^{-1}$, determined in our laboratory.

Penkett *et al.* measured the activation energy of Reaction (1) in early time. Their results under different pH are $E_a$=30.39 kJ. $mol^{-1}$ when pH=4.6 and $E_a$=38.58 kJ. mol $^{-1}$ when pH=6.6. It is obtained by using extension method that when pH=4.0 $E_a$=27.48 kJ. $mol^{-1}$, which is 4.6% lower than that of our work. Because the correlation of log $k^{(2)}$ with pH obtained through early work of Penkett *et al.* is inconsistent with HE mechanism, the activation energy measured in our laboratory might be more credible.

3.3 Effect of formaldehyde on $H_2O_2$-S(IV) reaction rate

Formaldehyde, an important atmospheric species both as a primary pollutant and a photochemical reaction product, has been found to be present in the gas phase as well as in precipitation. The concentration of formaldehyde in hydrometers was up to 2 mg/L (corresponding to 67μmol/L; Yusuf, 1984), with a volume-weighted average concentration of approximately 6 μmol/L (Lee, 1986). Formaldehyde can react with S(IV) in aqueous solution to form adduct hydroxymethanesulfonic acid (abbreviated to HMSA); this adduct is stable with respect to oxidation by hydrogen peroxide and decomposes extremely slowly to HCHO and S(IV) (Kok, 1986). In order to clarify the relation between formaldehyde and $H_2O_2$-S(IV) reaction, we conducted the experimental kinetics studies and model calculations about the effect of formaldehyde on $H_2O_2$-S(IV) reaction.

3.3.1 Kinetic studies in laboratory

Experimental procedures were identical to those in purified water, with a difference that hydrogen peroxide and formaldehyde were added to the reaction cell before $NaHSO_3$ was added to initiate the reaction. The results of linear regression of $\log k^{(2)}$-pH were listed in Table 1, including the results obtained in purified water; the third-order rate constants are listed in Table 2.

**Table 1 The linear regression results of $\log k^{(2)}$-pH determined in formaldehyde solution and purified water respectively**

| [HCHO], μmol/L | Expression formulae | Correlation coefficience |
|---|---|---|
| 0 | $\log k^{(2)} = (8.05 \pm 0.03) - (1.006 \pm 0.006)$pH | −0.9995 |
| 20 | $\log k^{(2)} = (8.05 \pm 0.03) - (1.008 \pm 0.006)$pH | −0.9997 |
| 60 | $\log k^{(2)} = (8.03 \pm 0.04) - (1.001 \pm 0.010)$pH | −0.9992 |

**Table 2 The third-order rate constants determined in formaldehyde solution and purified water respectively**

| [HCHO], μmol/L | $k^{(3)}$, $(\text{mol/L})^{-2} \cdot s^{-1}$ | $\log k^{(3)}$ |
|---|---|---|
| 0 | $(1.06 \pm 0.05) \times 10^8$ | $8.02 \pm 0.02$ |
| 20 | $(1.05 \pm 0.04) \times 10^8$ | $8.02 \pm 0.02$ |
| 60 | $(1.05 \pm 0.06) \times 10^8$ | $8.02 \pm 0.03$ |

Here it should be pointed out that the rate constants under three conditions were completely identical within the experimental error, the scatters in rate constants were equal, which at least suggests that effect of formaldehyde on Reaction (1) can not be observed for the concentration of formaldehyde range $0-60$ μmol/L.

For comparison, we try to calculate the rate of $H_2O_2$-S(IV) Reaction (5), in which $k^{(3)}=1.06\times10^8$ $(mol/L)^{-2}S^{-1}$ (determined in our laboratory), and the rate of S(IV)-HCHO reaction

$$-\frac{d\ [S(IV)]}{dt}=k_f\ [HCHO]\ [S(IV)], \tag{9}$$

the values of $k_f$ corresponding to different pH are listed in Table 3.

**Table 3 The $k_f$ values under different pH**

| pH | 2 | 3 | 4 | 5 |
|---|---|---|---|---|
| $k_f$ | 0.308 | 1.21 | 1.94 | 12.6 |
| Ref. | a | | b | |

Note: a: Boyce, 1984; b: Kok, 1986

The results of the reaction rates calculation with respect to Equation (5) and (9) are listed in Table 4.

**Table 4 The results of the parallel rates calculation with respects to Equation (5) and (9) ($t=25$ ℃, $[H_2O_2]_0=[S\ (IV)]_0=4\mu mol/L$)**

| Reaction | pH 2 | 3 | 4 | 5 |
|---|---|---|---|---|
| | Rate of reaction, mol/L. $S^{-1}$ | | | |
| $S(IV)+H_2O_2\longrightarrow$ S(VI) | $1.70\times10^{-5}$ | $1.70\times10^{-6}$ | $1.70\times10^{-7}$ | $1.70\times10^{-8}$ |
| | | [HCHO] = 6μmol/L | | |
| $S(IV)+HCHO\xrightarrow{HMSA}$ | $7.39\times10^{-12}$ | $2.90\times10^{-11}$ | $4.65\times10^{-11}$ | $3.02\times10^{-10}$ |
| | | (1)/(2) | | |
| | $2.3\times10^{6}$ | $5.86\times10^{4}$ | $3.66\times10^{3}$ | 56.3 |
| | | [HCHO] = 60μmol/L | | |
| | $7.39\times10^{-11}$ | $2.90\times10^{-10}$ | $4.65\times10^{-10}$ | $3.02\times10^{-9}$ |
| | | (1)/(2) | | |
| | $2.3\times10^{5}$ | $5.86\times10^{3}$ | $3.66\times10^{2}$ | 5.63 |

It is evident that the rate of S(IV)-$H_2O_2$ reaction was far faster than that of S (IV)-HCHO reaction which suggests that formaldehyde exerts little influence on the S (IV)-$H_2O_2$ reaction for the concentrations of formaldehyde range 0 – 60 μmol/L.

3.3.2 Model calculation

First let us to explain the meanings and units of the following nomenclature:

*a:* ionization fraction of S(IV) species; *p*: gas-phase $SO_2$ partial pressure, ppb; $H^*$: effective Henry's Law constant, mol/L. $atm^{-1}$; *L*: liquid water content, volume fraction; *dp/dt:* macroscopic removal rate of $SO_2$, %. $h^{-1}$; *R*: universal gas constant, 1. $atm^{-1}$. mol/L and

$$a_0 = \frac{[SO_2(aq)]}{[S(IV)]} = \frac{[H^+]^2}{[H^+]^2 + k_{a1}[H^+] + k_{a1}k_{a2}}$$

$$a_1 = \frac{[HSO_3^-]}{[S(IV)]} = \frac{k_{a1}[H^+]}{[H^+]^2 + k_{a1}[H^+] + k_{a1}k_{a2}}$$

$$a_2 = \frac{[SO_3^{2-}]}{[S(IV)]} = \frac{k_{a1}k_{a2}}{[H^+]^2 + k_{a1}[H^+] + k_{a1}k_{a2}}$$

The constants being used in the following calculation are listed in Table 5.

**Table 5 Henry's Law constants, acid dissociation constants and reaction rate constants of $H_2O_2$, $SO_2$ and HCHO ($t$ = 25 ℃ )**

| Process | Constants | Ref. |
|---|---|---|
| $H_2O_2(g) \rightleftharpoons H_2O_2$ (aq) | $H_{H_2O_2} = 7.1 \times 10^4$mol/L.atm$^{-1}$ | *a* |
| $SO_2(g) \rightleftharpoons SO_2(aq)$ | $H_{SO_2} = 1.26$mol/L.atm$^{-1}$ | *b* |
| $SO_2.H_2O$ (aq) $\rightleftharpoons$ $H^+ + HSO_3^-$ | $Ka_1 = 1.45 \times 10^2$mol/L | *b* |
| $HSO_3^- \rightleftharpoons H^+ + SO_3^{2-}$ | $Ka_2 = 6.31 \times 10^{-3}$mol/L | *b* |
| $HCHO(g) + H_2O \rightleftharpoons CH_2(OH)_2$ | $H_{HCHO} = 2.97 \times 10^3$mol/L.atm$^{-1}$ | *b* |
| $CH_2(OH)_2 \rightleftharpoons HCHO + H_2O$ | $Kd = 5.5 \times 10^{-4}$ | *b* |
| $HCHO + HSO_3^- \rightarrow CH_2(OH)SO_3^-$ | $k_1 = 7.90 \times 10^2$(mol/L)$^{-1}$S$^{-1}$ | *b* |
| $HCHO + SO_3^{2-} \rightarrow CH_2(O^-)SO_3^-$ | $k_2 = 2.50 \times 10^7$(mol/L)$^{-1}$S$^{-1}$ | *b* |

Notes: a: Martain, 1981; b: Olson, 1989

3.4 Formula deduction

The reactions of dissolved S(IV) with $H_2O_2$ and HCHO were

$$S(IV)+H_2O_2\ (aq)\longrightarrow S(VI), \tag{1}$$

$$S(IV)+HCHO\ (aq)\longrightarrow HMSA, \tag{10}$$

respectively, through which the macroscopic $SO_2$ removal rates can be defined as (Olson, 1989)

$$\frac{dp}{dt}=3.6\times10^{14}\left(\frac{-d[S(IV)]/dt.\ L}{P_{SO_2}H_{SO_2}L/a_0+P_{SO_2}/RT}\right),$$

$$(\%.\ h^{-1}), \tag{11}$$

where $-d[S(IV)]/dt$ represents the rate of Reaction (1) or Reaction (10).

Macroscopic $SO_2$ removal rates due to the reaction of dissolved S(IV) with $H_2O_2$.

The rate of Reaction (1) for the pH range 3−6 is

$$-d[S(IV)]/dt=1.06\times10^{8}[H^+][S(IV)][H_2O_2], \tag{12}$$

where the rate constant adopted was measured in our laboratory.

We can get a pH independent rate at constant $SO_2$ pressure, i. e.,

$$-d[S(IV)]/dt=1.54\times10^{-12}P_{H_2O_2}\ H_{H_2O_2}P_{SO_2}H_{SO_2}, \tag{13}$$

Fitting Equation (13) and corresponding constants to Equation (11), we get

$$dp/dt=3.9\times10^{7}P_{H_2O_2}\ \frac{L}{L+0.0325},\ (\%.\ h^{-1}) \tag{14}$$

Equation (14) is just macroscopic $SO_2$ removal rate due to the reaction of dissolved S(IV) with $H_2O_2$ at temperature 25 ℃ .

Macroscopic $SO_2$ removal rate due to the reaction of dissolved S(IV) with HCHO to form adduct HMSA.

The rate of Reaction (10) is (Boyce, 1984)

$$-d[S(IV)]/dt=(k_1a_1+k_1a_1)\frac{K_a}{K_a+1}\ [S(IV)][HCHO]_t, \tag{15}$$

where $[HCHO]_t=[HCHO]+[CH_2(OH)_2]$.

$[S(IV)]=[SO_2(aq)]/a_0$. Supposing $x$ ppb gaseous $SO_2$ dissolved in water, then

$$\underset{(P_{SO_2}-x).10^{-9}}{SO_2(g)} \xrightleftharpoons{H_{SO_2}} \underset{[SO_2(aq)]}{SO_2(aq)}$$

For equilibrium

$$H_{SO_2}=\frac{[SO_2\ (aq)]}{(P_{SO_2}-x).\ 10^{-9}}\cdot 10^9,$$

therefore

$$x=P_{SO_2}-\frac{[SO_2\ (aq)]}{H_{SO_2}}.$$

According to material balance $x.\ H_{SO_2}10^{-9}=[S(IV)]$, through which we calculated to get

$$[S(IV)]=\frac{1}{1+a_0}\cdot 10^{-9}\cdot H_{SO_2}P_{SO_2}. \tag{16}$$

Supposing $y$ ppb gaseous formaldehyde dissolve in water, then

$$\underset{(p_{HCHO}-y).\ 10^{-9}}{HCHO\ (g)+H_2O} \xrightleftharpoons{H^*_{HCHO}} \underset{[CH_2(OH)_2]}{CH_2(OH)_2\ (aq)}$$

$$\underset{[CH_2(OH)_2]}{CH_2(OH)_2\ (aq)} \xrightleftharpoons{k_d} \underset{[HCHO]}{HCHO\ (aq)+H_2O}$$

For equilibrium

$$[HCHO]=K_d\ [CH_2(OH)_2]$$

$$[CH_2(OH)_2]=(P_{HCHO}-y)H^*_{HCHO}\cdot\ 10^{-9}$$

According to material balance

$$[HCHO]_t = [HCHO] + [CH_2(OH)_2] = y \cdot 10^{-9} \cdot H^*_{HCHO}$$

therefore

$$[HCHO]_t = \frac{k_d + 1}{k_d + 2} \cdot 10^{-9} \cdot P_{HCHO} H^*_{HCHO}, \quad (17)$$

fitting Equations (16), (17) and constant $K_d$ to Equation (15), we get

$$-d[S(IV)]/dt = 2.75 \times 10^{-22} \frac{k_1 a_1 + k_2 a_2}{1 + a_0} H_{SO_2} P_{SO_2} H^*_{HCHO} P_{HCHO}, \quad (18)$$

fitting Equations (18) to (11), we get

$$dp/dt = 2.94 \times 10^{-4} (k_1 a_1 + k_2 a_2) \frac{a_0}{1 + a_0} P_{HCHO} \frac{L}{L + 0.0325}, (\%. h^{-1}). \quad (19)$$

Formula (19) is just macroscopic $SO_2$ removal rate due to the reaction of dissolved S(IV) with HCHO to form adduct HMSA.

3.5 Calculation results

Because clouds and fogs contain the liquid water contents range $0.01 - 1 ml.m^{-3}$, we adopt $L = 10^{-6}$ ($1ml.\ m^{-3}$) and $L = 10^{-8}$ ($0.01\ ml.\ m^{-3}$) in our calculations. The calculation results are listed in Table 6 and Table 7.

**Table 6 Macroscopic $SO_2$ removal rates due to the reaction of dissolved S(IV) with $H_2O_2$ ($t = 25$ ℃, $P_{H_2O_2} = 1ppb$)**

| Change ratio | $L$ | |
|---|---|---|
| | $10^{-6}$ | $10^{-8}$ |
| $dp/dt$, $P_a$, $h^{-1}$ | 1200 | 12 |
| log ($dp/dt$) | 3.08 | 1.08 |

log ($dp/dt$) − pH are plotted in Fig. 8.

It should be noted in Fig. 8 that macroscopic removal rates of $SO_2$ due to oxidation by $H_2O_2$ were far faster than those due to reaction with HCHO to form HMSA which suggests that formaldehyde with typical atmospheric concentration exerts no influence on the reaction of dissolved S (IV) with $H_2O_2$ in the pH range characteristic of cloud water and precipitation, and within the typical liquid water

**Table 7 Macroscopic $SO_2$ removal rates due to the reaction of dissolved S(IV) with HCHO to form adduct HMSA ($t$=25℃, $P_{HCHO}$=10ppb)**

| | pH | | | | |
|---|---|---|---|---|---|
| | 2 | 3 | 4 | 5 | 6 |
| | | | $dp/dt$, $P_o.h^{-1}$ | | |
| $L$ | | | | | |
| $10^{-6}$ | $3.60\times10^{-5}$ | $-1.87\times10^{-4}$ | $1.46\times10^{-3}$ | $1.35\times10^{-2}$ | 0.09 |
| $10^{-8}$ | $3.60\times10^{-7}$ | $1.87\times10^{-6}$ | $1.47\times10^{-5}$ | $1.41\times10^{-4}$ | $1.32\times10^{-3}$ |
| | | | Log (de/dt) | | |
| $10^{-6}$ | −4.44 | −3.73 | −2.84 | −1.87 | −1.05 |
| $10^{-8}$ | −6.44 | −5.73 | −4.83 | −3.85 | −2.88 |

content range of fogs and clouds.

Both kinetic studies in laboratory and model calculations demonstrated that the oxidation of S(IV) by $H_2O_2$ is sufficiently faster than complexation of S (IV) with HCHO, therefore the latter reaction would not represent an interference to the former.

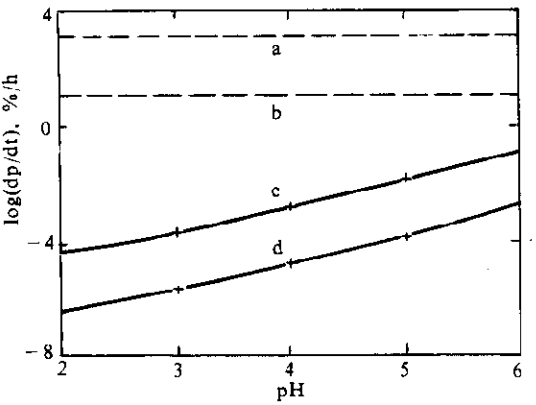


Fig. 8 Solid lines: macroscopic removal rates, $dp/dt$, of $SO_2$ from the atmosphere due to HMSA formation for two liquid water contents $L$. Doted lines: macroscopic removal rates of $SO_2$ due to oxidation by $H_2O_2$ ($P_{HCHO}$=10ppb, $P_{H_2O_2}$=1ppb)
a. $L=10^{-6}$ b. $L=10^{-8}$ c. $L=10^{-6}$ d. $L=10^{-8}$

## 4 Conclusions

To some extent that kinetics in precipitation is representative of kinetics in clouds, the results obtained here, i. e., scatter of ±17.3% in the $H_2O_2$-S(IV) rate with a positive bias of 4% in precipitation with respect to the rate in purified water would imply an equivalent effect on rates in cloud. Because the rate of oxidation of dissolved S(IV) by $H_2O_2$ is very fast, and this reaction is not a rate-limiting procedure in some processes of the atmospheric acid formation, the applicatility of the kinetic results obtained with purified water to model calculations about rain and cloud for the assessment of the contribution of Reaction (1) to atmospheric $SO_2$ oxidation is therefore considered to be justified, the small positive bias observed on the kinetics of this reaction is not expected to exert

an appreciable effect on atmospheric $SO_2$ oxidation in precipitation.

**Acknowledgements**— The authors thank the following individuals for help with various aspect of the field, laboratory research and calculation: Zhao Qianxue and Zhang Baozhu.

## References

Boyce Scott D, Hoffmann Michael R. J Phys Chem, 1984; 88:4740

John H Ovreton Jr. Atmos Environ, 1985; 19:687

Kunen SM, Lazrus A, L Kok GL, Heikes BG. J Geophys Res, 1983; 88C(6):3671

Kok Gregory L, Gitlin Sonia N, Lazrus Allan L. J Geophys Res, 1986; 91(D):2801

Lee Y-N, Shen J, Klotz PJ, Schwartz SE, Newman L. J Geophys Res, 1986; 91D(12), 13:264

Olson Terese M, Hoffmann Michael R. Atmos Environ, 1989; 23(5):985

Penkett SA, Jones BMR, Brice KA, Eggleton AEG. Atmos Environ, 1979; 13:123

Robbin L Martain, Donald E Damschen. Atmos Environ, 1981; 15(9):1615

Yusuf Gbadebo Adewuyi, Cho Seog-Yeon, Tsay Re-Peng, Gregory R Carmichael. Atmos Environ, 1984; 18(11):2413

(Received November 20, 1991)